

Supplementary Information to: *Voltage breakdown analyses in anion exchange membrane water electrolysis – the contributions of catalyst layer resistance on overall overpotentials*

Emily K. Volk¹, Elliot Padgett², Melissa E. Kreider², Stephanie Kwon^{3*}, Shaun M. Alia^{2*}

¹Advanced Energy Systems Graduate Program, Colorado School of Mines, Golden
Colorado 80401, United States

²Chemistry and Nanoscience Center, National Renewable Energy Laboratory, Golden,
Colorado 80401, United States

³Department of Chemical and Biological Engineering, Colorado School of Mines,
Golden, Colorado 80401, United States

* Corresponding authors: shaun.alia@nrel.gov, kwon@mines.edu

Experimental Methods

Catalytic materials. Catalyst materials were obtained from commercial suppliers and used without further treatment. IrO_2 (Alfa Aesar, 99.99%), Mn_2O_3 (US Research Nanomaterials Inc., 99.2%), Co_3O_4 (US Research Nanomaterials Inc.), NiFe_2O_4 (US Research Nanomaterials Inc.); cathode catalyst: Pt on C support (47% Pt, Tanaka Kikinzoku Kogyo, TEC10E50E). Pt/C was employed as the cathode catalyst to reduce cathode-induced variability and enable clearer attribution of performance trends to changes in the OER catalyst layer.

Electrochemical testing. All RDE experiments were performed in a Teflon cell with Au mesh counter electrode, Hg/HgO reference electrode, and catalysts deposited on Au discs as working electrodes. RDE tests were performed in 0.1 M NaOH (Sigma-Aldrich, TraceSELECT grade, 99.9995%). All MEA experiments were performed using a two-electrode configuration and reported potentials are cell potentials. MEA experiments were performed in 1 M KOH (EMD Millipore, Emsure grade) at 80 °C. An Autolab PGSTAT302N potentiostat (Eco Chemie, Metrohm Autolab) was used for all electrochemical measurements for both MEA and RDE testing (including polarization curves, cyclic voltammetry, and electrochemical impedance spectroscopy).

Rotating disc electrodes (RDEs). RDE inks were formulated to target 100 $\mu\text{g}/\text{cm}^2$ on the Au working electrodes in inks containing 76 vol% DIW and 24 vol% nPA with 10 wt% of Nafion was used as a binding agent.

Membrane electrode assemblies (MEAs). Single-cell MEAs with a 5 cm^2 active area and consisting of a carbon paper gas diffusion layer (Fuel Cell Earth, MGL280, 80280-40) on the cathode side, a catalyst-coated Ni mesh porous transport layer on the anode side (Bekaert BEKIPOR 2NI 19-0.25), and Versogen 80 μm membranes were utilized for all tests. Cathode catalyst layers were composed of Pt/C with 30 wt% of the Versogen polymer and deposited as either CCM or CCS depending on the project (refer to the source publication as indicated). Anode ink dispersions were formulated to target 0.5 mg cm^2 of catalyst (metal) and 30 wt% Versogen PiperION TP-85 Ionomer (5 wt% dispersion in ethanol) and consisted of 10 vol% deionized water (DIW) and 90 vol% n-propanol. Cathode catalyst layers were directly sprayed

onto Versogen PiperION membranes (TP-85, 80 μm) using a Sonotek spray station with Accumist nozzle. Cathode ink solutions were formulated to target 0.3 mg cm^{-2} of Pt and 30 wt% Versogen PiperION-A TP-85 ionomer solution and consisted of 57 vol% DIW and 43 vol% n-propanol. Cell hardware contained endplates (Fuel Cell Technologies), Au coated current collectors, and Ni triple serpentine flow fields. Membranes were pretreated via soaking in 3 M KOH for 48 h (refreshed once at 24 h) and the catalyst-coated Ni mesh transport layers were pretreated via soaking in 3 M KOH for 24 h before use.

In this work, $T = 80\text{ }^{\circ}\text{C}$ and P_{O_2} and P_{H_2} are both 82.2 kPa (atmospheric pressure in Denver, CO), yielding a standard cell potential of $E_o = 1.18\text{ V}$.

Theory – effective Tafel kinetics

The single-electrode Tafel approximation can be written:

$$\eta = b \log_{10} \left(\frac{J}{J_0} \right)$$

For overpotential η , Tafel slope b , current J , and exchange current density J_0 . For a two electrode cell, with each electrode following Tafel kinetics, we have:

$$\begin{aligned} \eta_{tot} &= b_1 \log_{10} \left(\frac{J}{J_1} \right) + b_2 \log_{10} \left(\frac{J}{J_2} \right) \\ &= (b_1 + b_2) \log_{10} (J) - (b_1 \log_{10} (J_1) + b_2 \log_{10} (J_2)) \\ &= (b_1 + b_2) \log_{10} (J) - (b_1 + b_2) \left(\frac{b_1}{(b_1 + b_2)} \log_{10} (J_1) + \frac{b_2}{(b_1 + b_2)} \log_{10} (J_2) \right) \\ &= b_{eff} \log_{10} (J) - b_{eff} \left(\log_{10} \left(J_1^{b_1/b_{eff}} \right) + \log_{10} \left(J_2^{b_2/b_{eff}} \right) \right) \\ &= b_{eff} \log_{10} \left(\frac{J}{J_1^{b_1/b_{eff}} J_2^{b_2/b_{eff}}} \right) \\ &= b_{eff} \log_{10} \left(\frac{J}{J_{0,eff}} \right) \end{aligned}$$

For $b_{eff} = b_1 + b_2$ being the “effective” Tafel slope, and $J_{0,eff} = J_1^{b_1/b_{eff}} J_2^{b_2/b_{eff}}$

So, it is valid to use an “effective Tafel approximation” for analysis of kinetics in two-electrode cells, provided that each electrode follows Tafel kinetics.

Theory – catalyst layer resistance

As discussed in the section in Tafel kinetics, in the absence of a reference electrode and with the high cathodic overpotentials expected for alkaline HER, measured catalyst layer resistances are likely a combination of anode and cathode contributions. These can be modeled by using two transmission lines in series:

$$Z_{total} = Z_{an} + Z_{cat} = \frac{R_{CL, an}}{\sqrt{\Lambda_{an}} \tanh \sqrt{\Lambda_{an}}} + \frac{R_{CL, cat}}{\sqrt{\Lambda_{cat}} \tanh \sqrt{\Lambda_{cat}}}$$

Where Z_p is the total transmission line impedance assumed to be a sum of the anodic and cathodic impedances, $R_{CL, an}$ and $R_{CL, cat}$ are the catalyst layer resistances of the anode and cathode, respectively and Λ_{an} and Λ_{cat} are the ratios of the resistive and capacitive components of the pore impedance:

$$\Lambda = \frac{R_{CL}}{Z_C}$$

Where the capacitive impedance Z_C is given by:

$$Z_C = \frac{1}{i\omega C_{DL}}$$

Where i is the imaginary number, ω is the frequency of the AC voltage, and C_{DL} is the double layer capacitance. The anode and cathode will each have their own C_{DL} .

In AEMWE, which is operated in supporting electrolyte, it is further possible for the transport layer itself to have a significant catalyst layer resistance. The transport layer substrates employed in AEMWE, often Ni or stainless steel based, are themselves OER active when flooded with supporting electrolyte and would need to be represented by additional terms with different boundary conditions. This is an important avenue for future work.

Additional Electrochemical Data

There was generally a negligible relationship between the high frequency resistance and catalyst layer construction/operational variables (catalyst loading, transport layer porosity, ionomer content, electrolyte concentration) as seen in **Figure S1**.

There were relationships between the electrochemical performance and the catalyst layer construction/operational variables (catalyst loading, transport layer porosity, ionomer content,

electrolyte concentration) as seen in **Figure S2**. These trends followed those of the R_{CL} ; i.e., compositions with low RCL also had high electrochemical activity (low overpotentials). Additional information on the full voltage breakdown analyses and mass activities are available from the source publications as referenced in the main text.

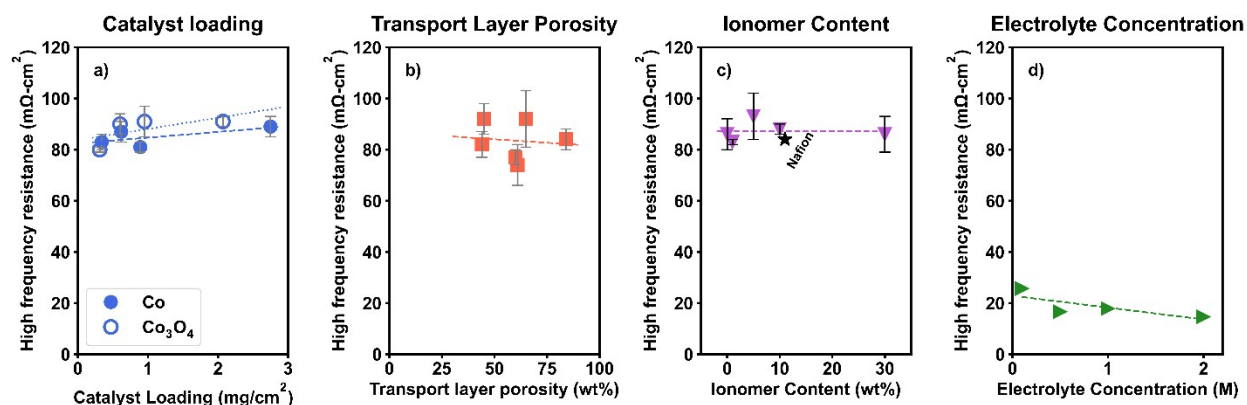


Figure S1. Impact of a) Co and Co_3O_4 catalyst loading, b) PTL porosity, c) ionomer content, and d) KOH supporting electrolyte concentration on HFR. All results are for changes to the anode catalyst layer only. Dashed lines are guides for the eye. In subfigures a-c, the average and standard deviation of three experiments are plotted as the markers and error bars, respectively.

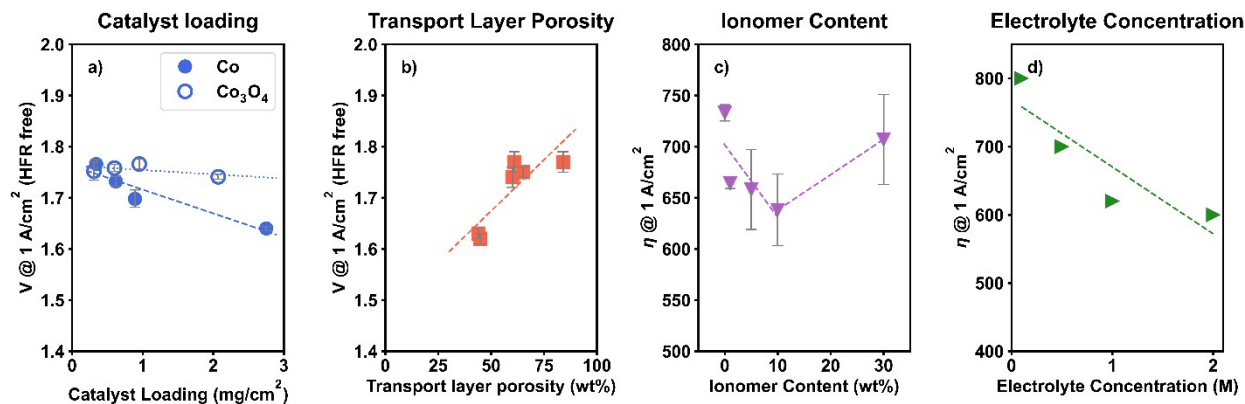


Figure S2. Impact of a) Co and Co_3O_4 catalyst loading, b) PTL porosity, c) ionomer content, and d) KOH supporting electrolyte concentration on activity. a) and b) show the HFR-free potential at $1 A/cm^2$ and c) and d) show the overpotential at $1 A/cm^2$. All results are for changes to the anode catalyst layer only. Dashed lines are guides for the eye. In subfigures a-c, the average and standard deviation of three experiments are plotted as the markers and error bars, respectively.